

Supporting information for
**Apoptotic Lysosomal Proton Sponge Effect in Tumor
Tissue by Cationic Gold Nanorods**

Dong Un Lee^{1,*}, Jun-Young Park^{1,2,*}, Song Kwon¹, Jun Young Park^{1,2}, Yong Ho Kim^{1,2,3}, Dongwoo Khang^{1,2,3,†}, and Jeong Hee Hong^{1,2,3,†}

¹*Lee Gil Ya Cancer and Diabetes Institute, Gachon University, Incheon 21999, South Korea*

²*Department of Health Sciences and Technology, GAIHST, Gachon University, Incheon 21999, Korea*

³*Department of Physiology, Gachon University, Incheon 21999, South Korea*

*equally contributed

†Corresponding authors e-mails: dkhang@gachon.ac.kr or minicleo@gachon.ac.kr

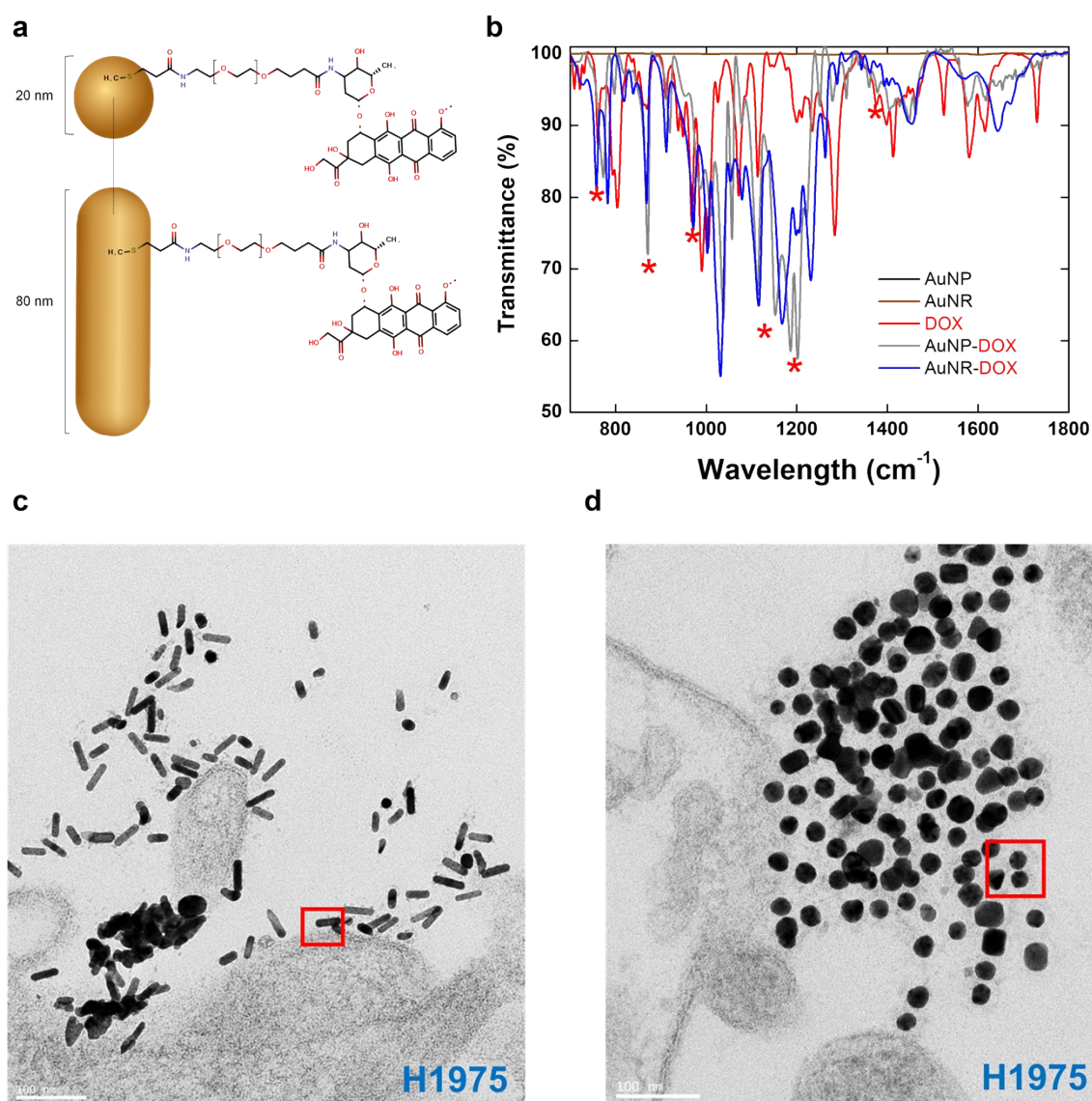


Figure S1. (a) Schematic illustration showing the covalently conjugated AuNP-DOX and AuNR-DOX. (b) FT-IR spectra showing that AuNP-DOX and AuNR-DOX have identical vibrational peaks that coincide with the DOX spectra as evidence of the successful covalent attachment of DOX to the AuNR and AuNP nanoparticles. (c-d) TEM images showing the AuNR-DOX and AuNP-DOX nanoparticles before cell entry (in cell culture media). The red square in the TEM images represents the magnified features of the covalently attached DOX corona on the AuNR and AuNP nanoparticles (Please see Fig. 1a for more detail). The scale bar represents 100 nm.

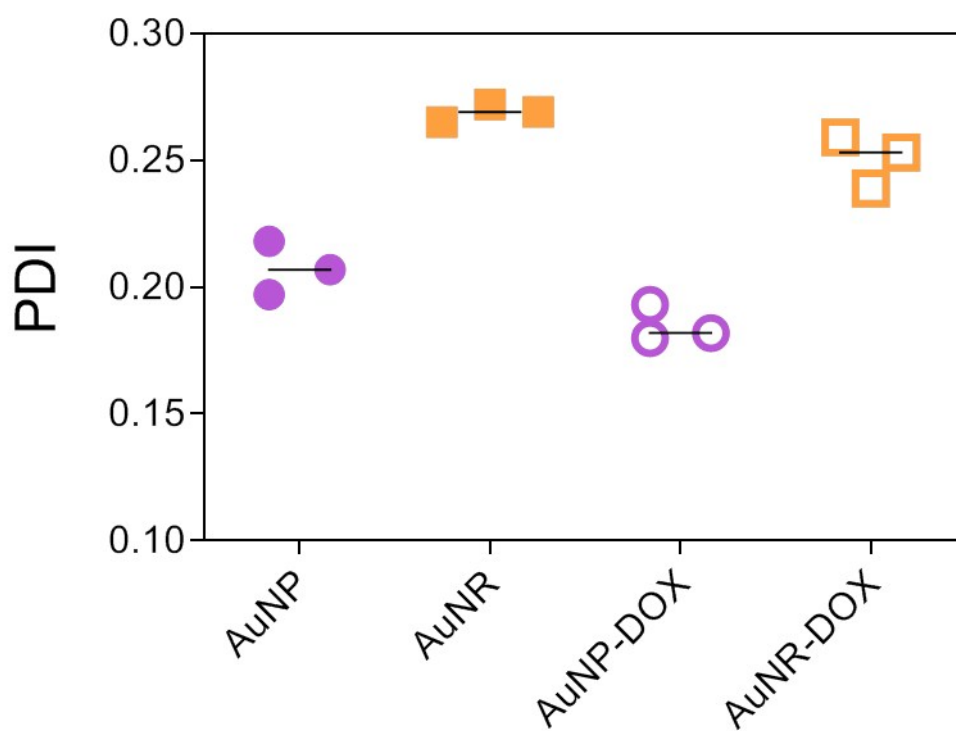


Figure S2. The polydispersity index (PDI) of AuNP (citrate), AuNR (CTAB), AuNP-DOX and AuNR-DOX after 10 days of the synthesis.

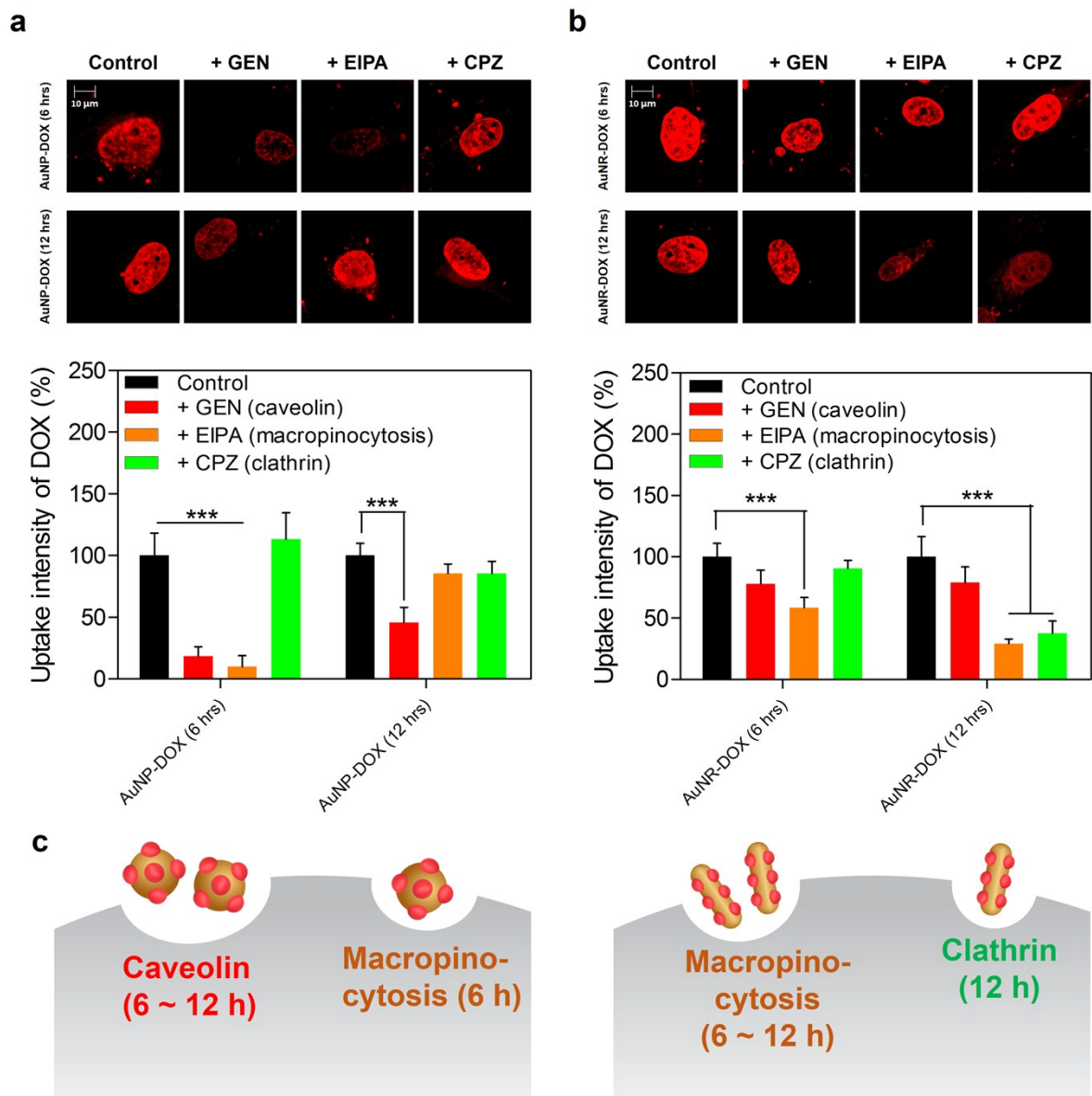
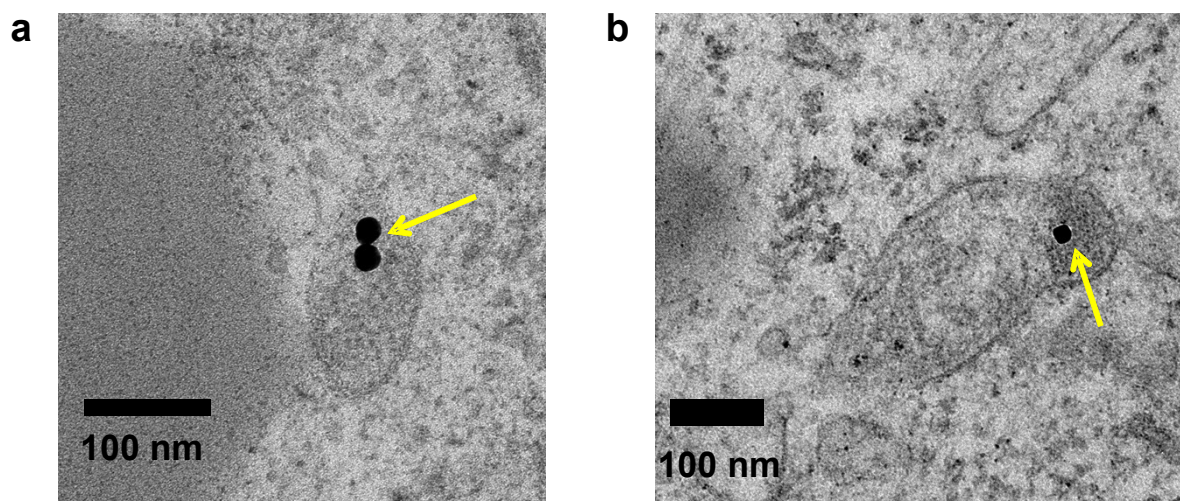
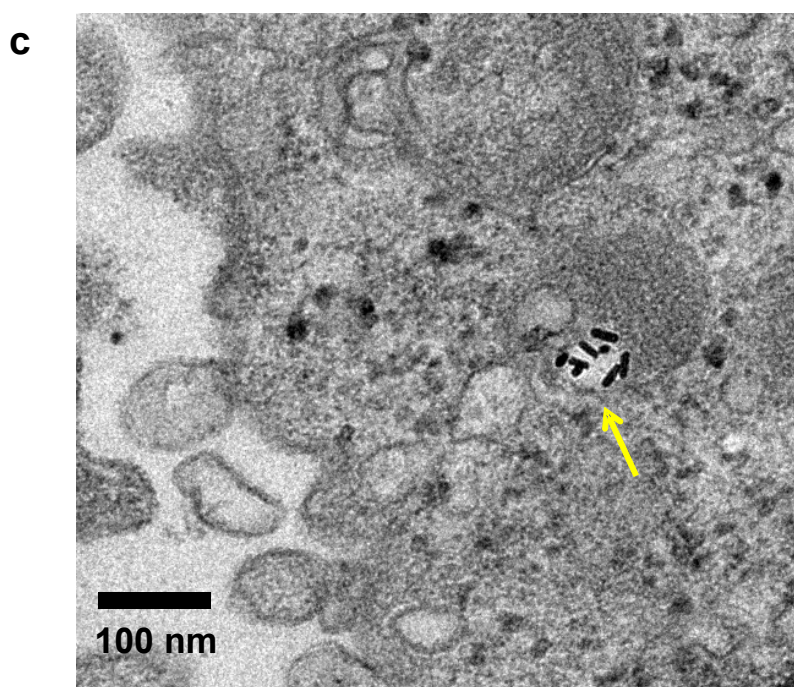


Figure S3. (a-b) Confocal analysis of DOX nuclear uptake in H1975 cells after treatment with endocytosis inhibitors (caveolin: GEN; micropinocytosis: EIPA; clathrin: CPZ) and AuNP-DOX and AuNR-DOX nanoparticles for 6 and 12 hrs. Data represent the mean \pm SEM (error bars) ($n = 3$), $**p < 0.01$ and $***p < 0.001$ compared with the control (no inhibitor). The scale bar represents 10 μ m. (c) Schematic illustration showing the main internalizing endocytic pathways used by the different Au nanodrugs (AuNP-DOX; caveolin and micropinocytosis, and AuNR-DOX; clathrin and macropinocytosis).



AuNP-DOX in H1975



AuNR-DOX in H1975

Figure S4. TEM images showing the internalized (a-b) AuNP-DOX and (c) AuNR-DOX in H1975 cell. The yellow arrow in the TEM images represents the internalized AuNP (a-b) and AuNR (c) nanoparticles in cellular compartment. The scale bars represent 100 nm.

Mitochondrial membrane potential (H1975)

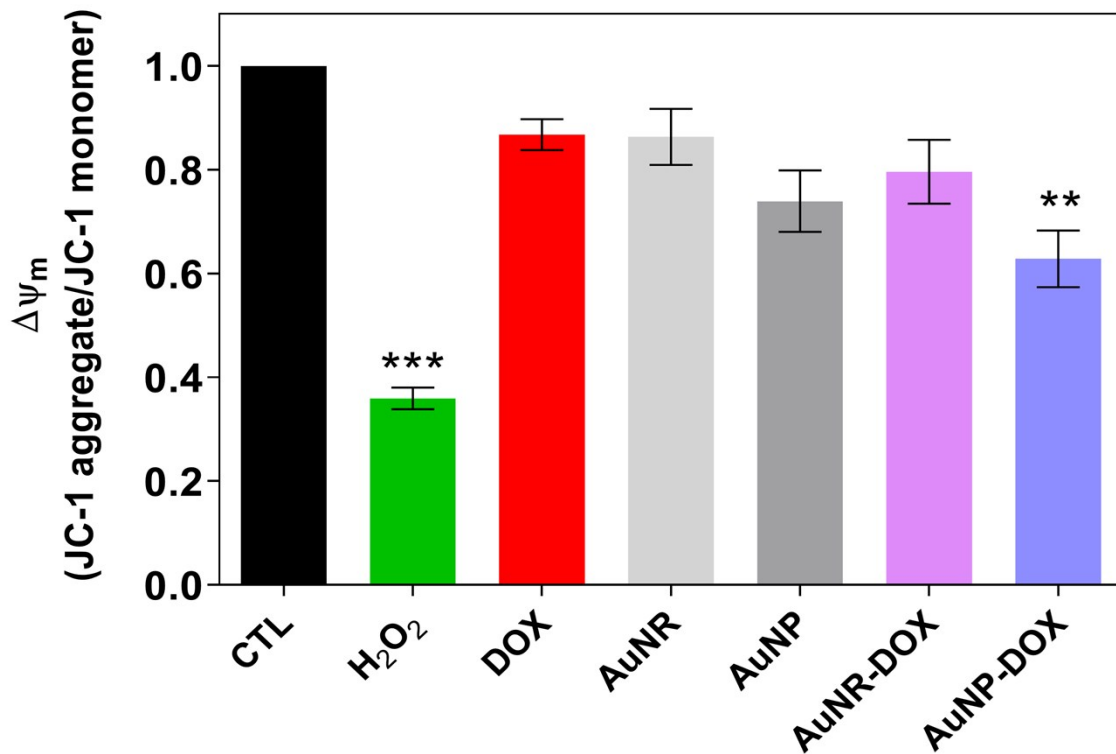


Figure S5. Changes in the mitochondrial membrane potential ($\Delta\Psi_m$) in H1975 cells after treatment with AuNR-DOX and AuNP-DOX. AuNR-DOX and AuNP-DOX did not significantly affect $\Delta\Psi_m$. Data represent the mean \pm SEM (error bars) ($n = 6$), ** $p < 0.01$ and *** $p < 0.001$ compared with the control.

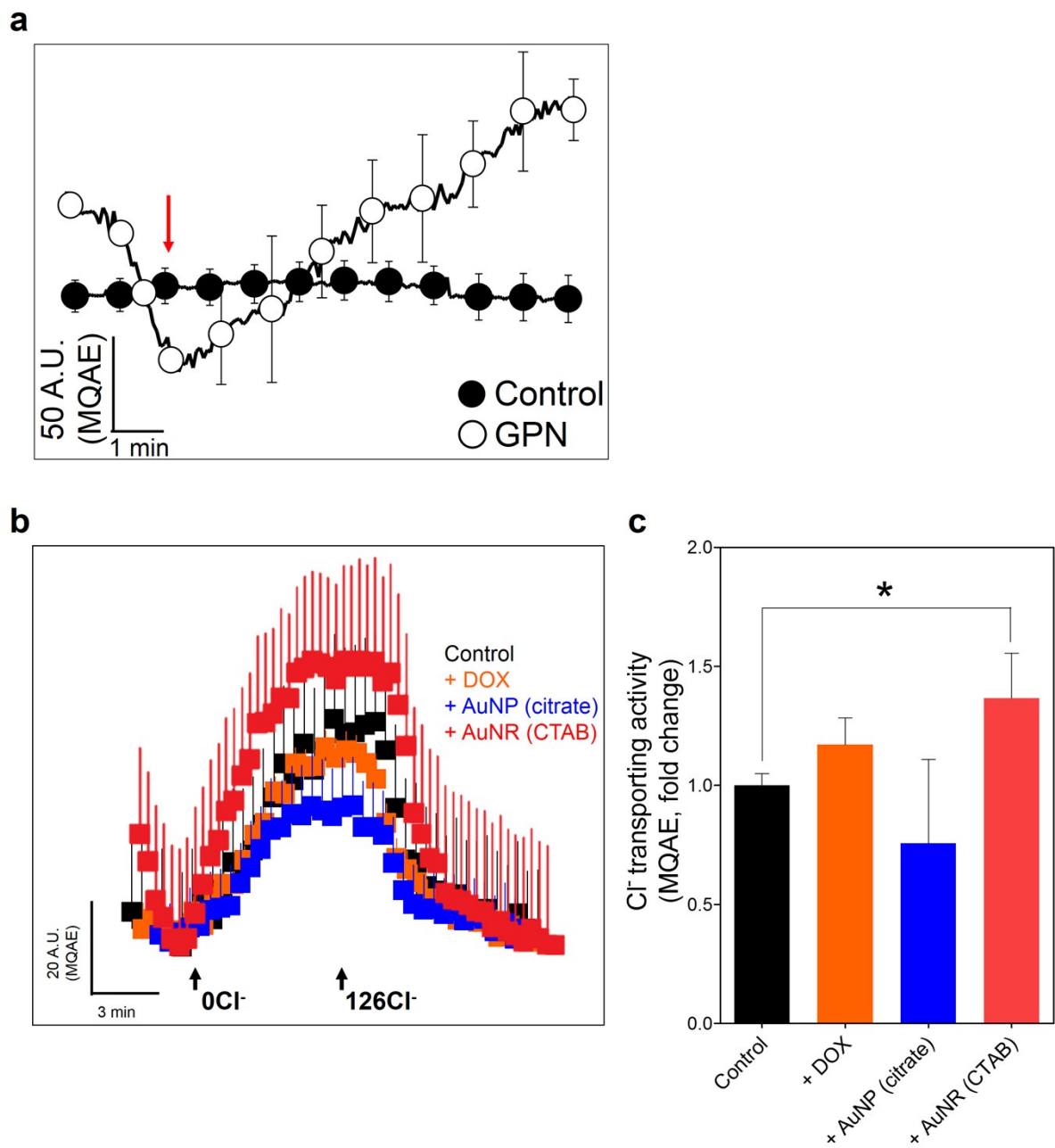
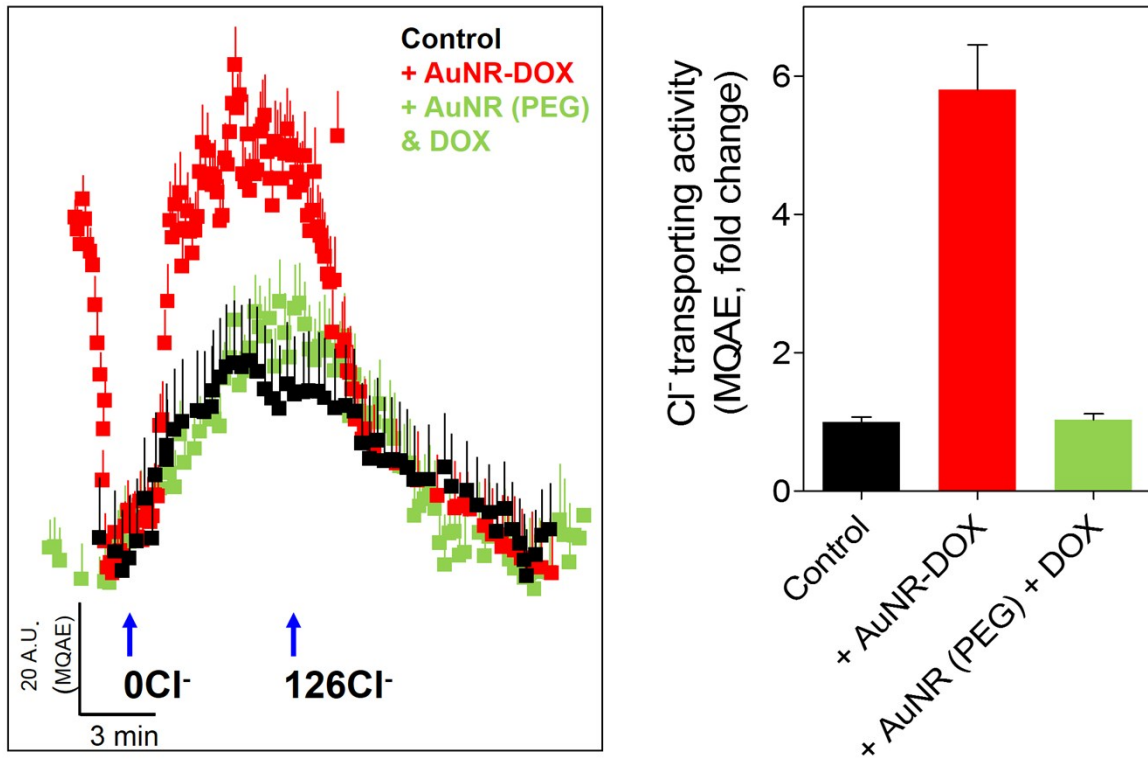


Figure S6. (a) Changes in Cl⁻ in H1975 cells after perfusing with GPN (400 μM) instead of 0Cl⁻ solution using MQAE fluorescence dye. (b) Changes in Cl⁻ in H1975 cells after treatment with DOX and cationic AuNRs (CTAB) or anionic AuNPs (citrate) for 24 hrs using MQAE fluorescence dye. (c) The data are presented as mean ± SEM (error bars) of the changes in Cl⁻.

a



b

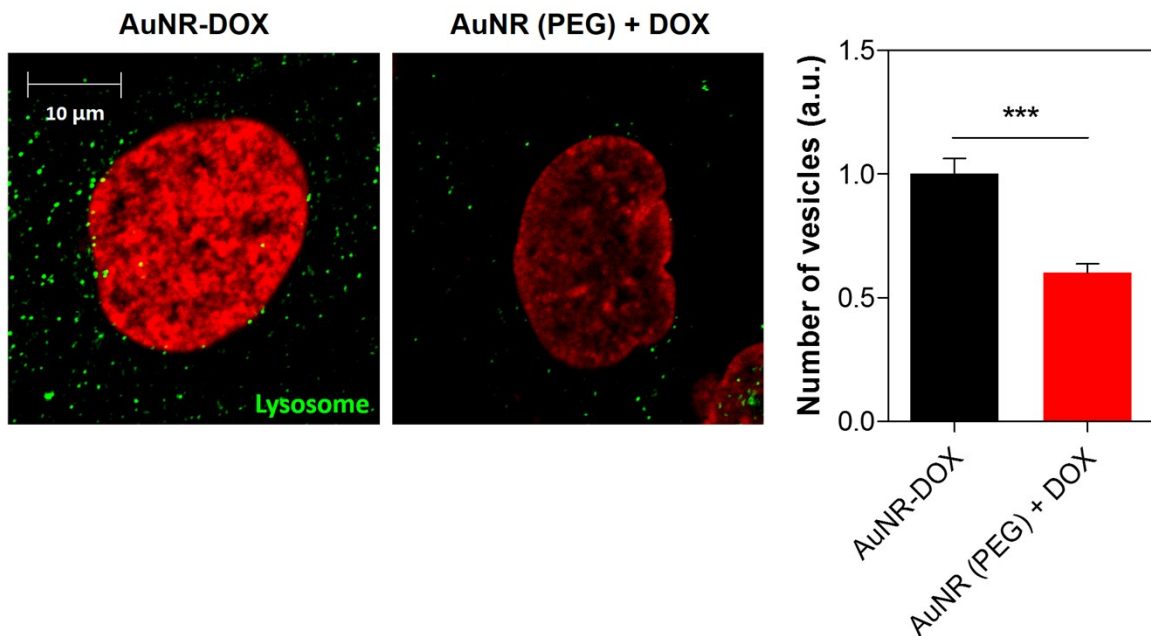


Figure S7. (a) Cl⁻ transporting activities by using the MQAE technique. H1975 cells were pretreated with AuNR conjugated DOX (AuNR-DOX) and with AuNR (PEG) mixed with DOX (AuNR (PEG) + DOX) for 24 hrs. Time course of the stimulated bath

solutions are represented with arrows. The activity was measured as the initial fluorescence increase in the 0 Cl⁻ bath solution. The bars are presented as means ± SEM. (b) Confocal microscopy of DOX (red) and lysosomal marker Rab 7 staining (green) in H1975 cells treated with AuNR-DOX and AuNR (PEG) + DOX for 24 hrs. The scale bar represents 10 μm. Data are presented as the mean ± SEM (error bars) of the relative number of vesicles (lysosomes) in the AuNR-DOX compared with the AuNR (PEG) + DOX (n = 3, ***p < 0.001).

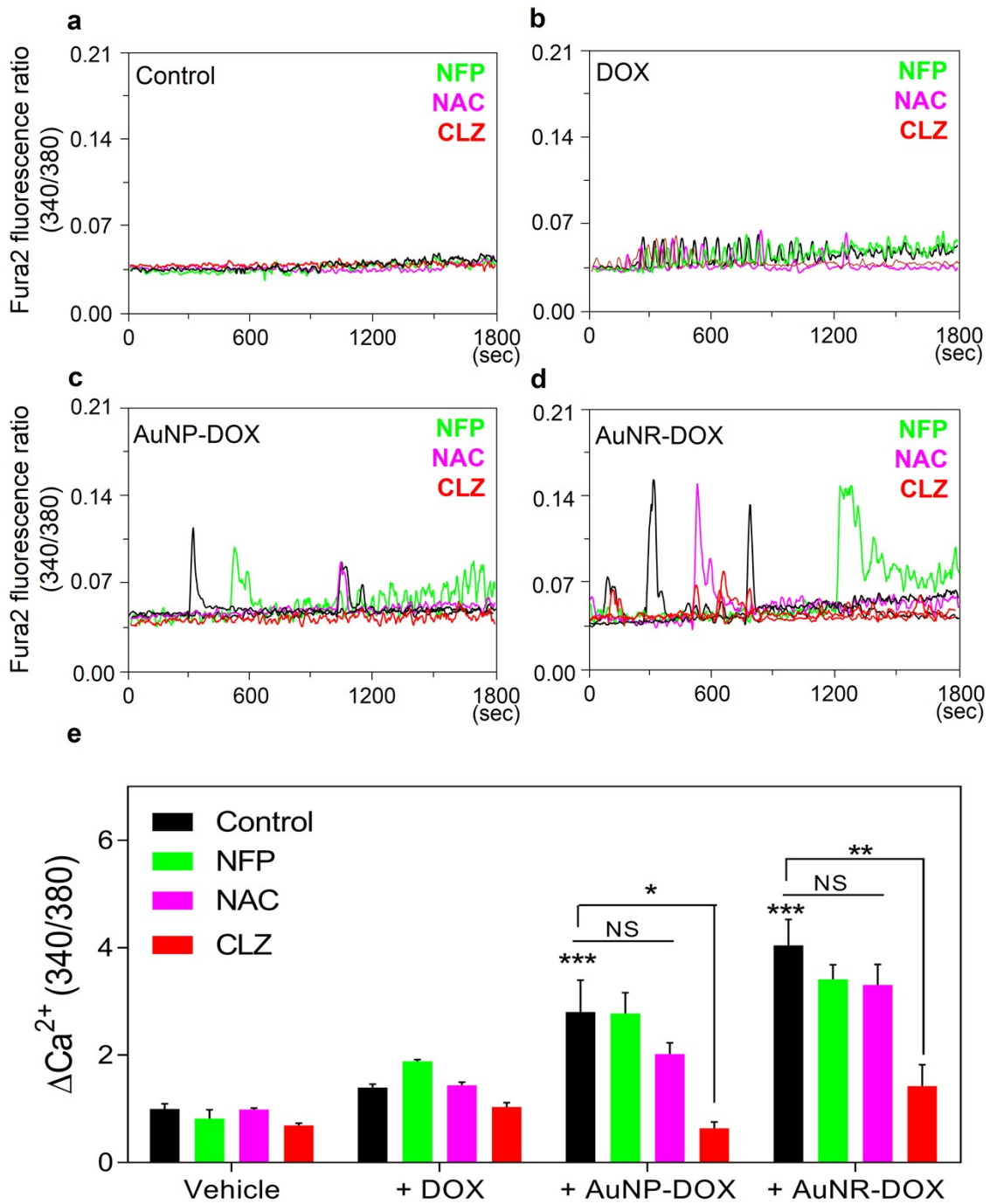


Figure S8. (a) Changes in $[Ca^{2+}]_i$ in control H1975 cells or H1975 cells treated for 24 hrs with AuNP (PEG) or AuNR (PEG) nanoparticles. (b) The data are shown as the mean \pm SEM (error bars) of $[Ca^{2+}]_i$ changes as determined using R340/380 fluorescence ratios, ** $p < 0.01$ and *** $p < 0.001$ compared with the control.

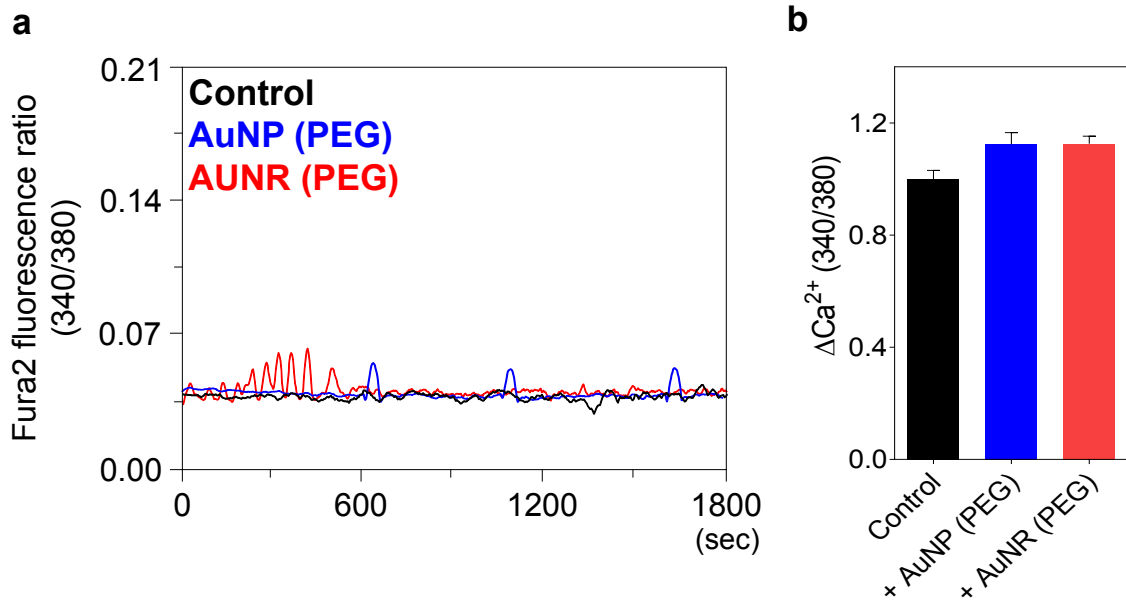


Figure S9. (a-d) $[Ca^{2+}]_i$ changes in control, DOX, AuNP-DOX, or AuNR-DOX treated H1975 cells with or without nifedipine (NFP, 10 μ M, green), NAC (5 mM, magenta), and clotrimazole (CLZ, 10 μ M, red) treatment. (e) Data are shown as the mean \pm SEM (error bars) of $[Ca^{2+}]_i$ changes (n = 3, NS; non-significant, *p < 0.05, **p < 0.01, ***p < 0.001).

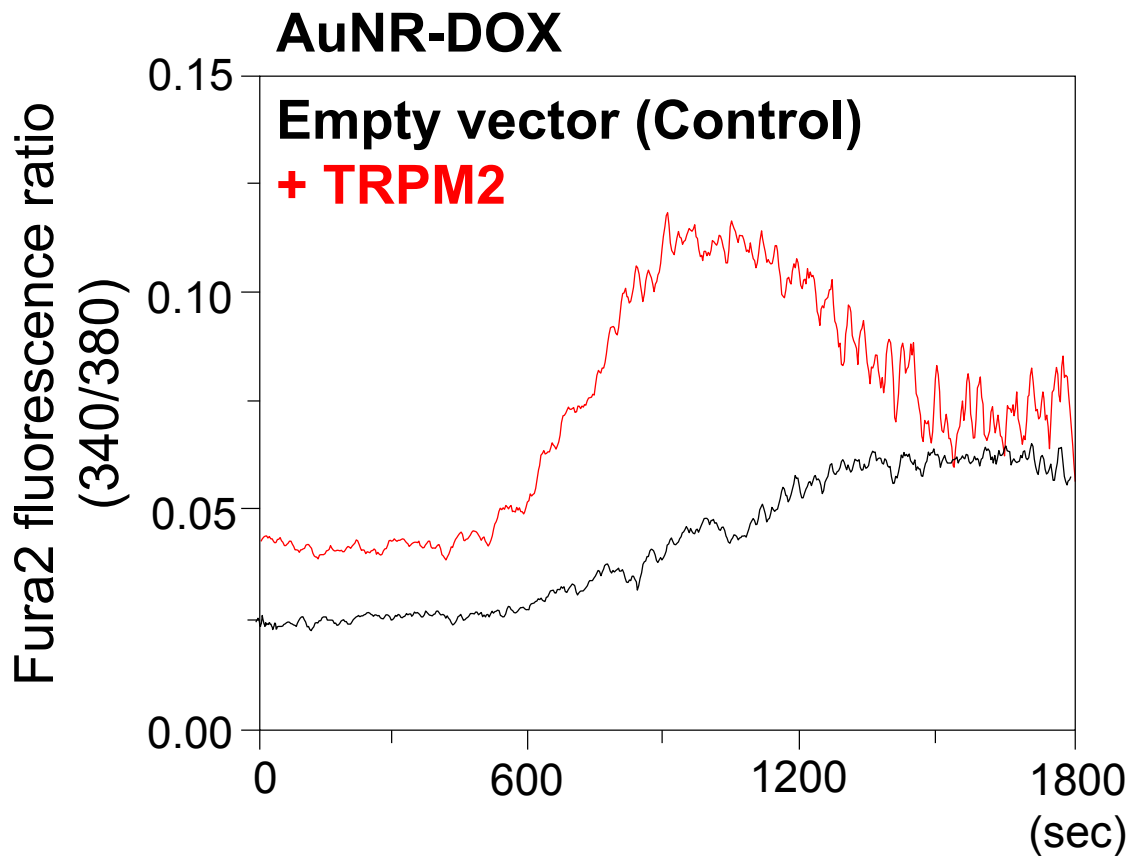


Figure S10. Changes in $[Ca^{2+}]_i$ induced by treatment with AuNR-DOX for 24 hrs in H1975 cells transfected with an empty vector (black) or a TRPM2 over-expressing plasmid (red).

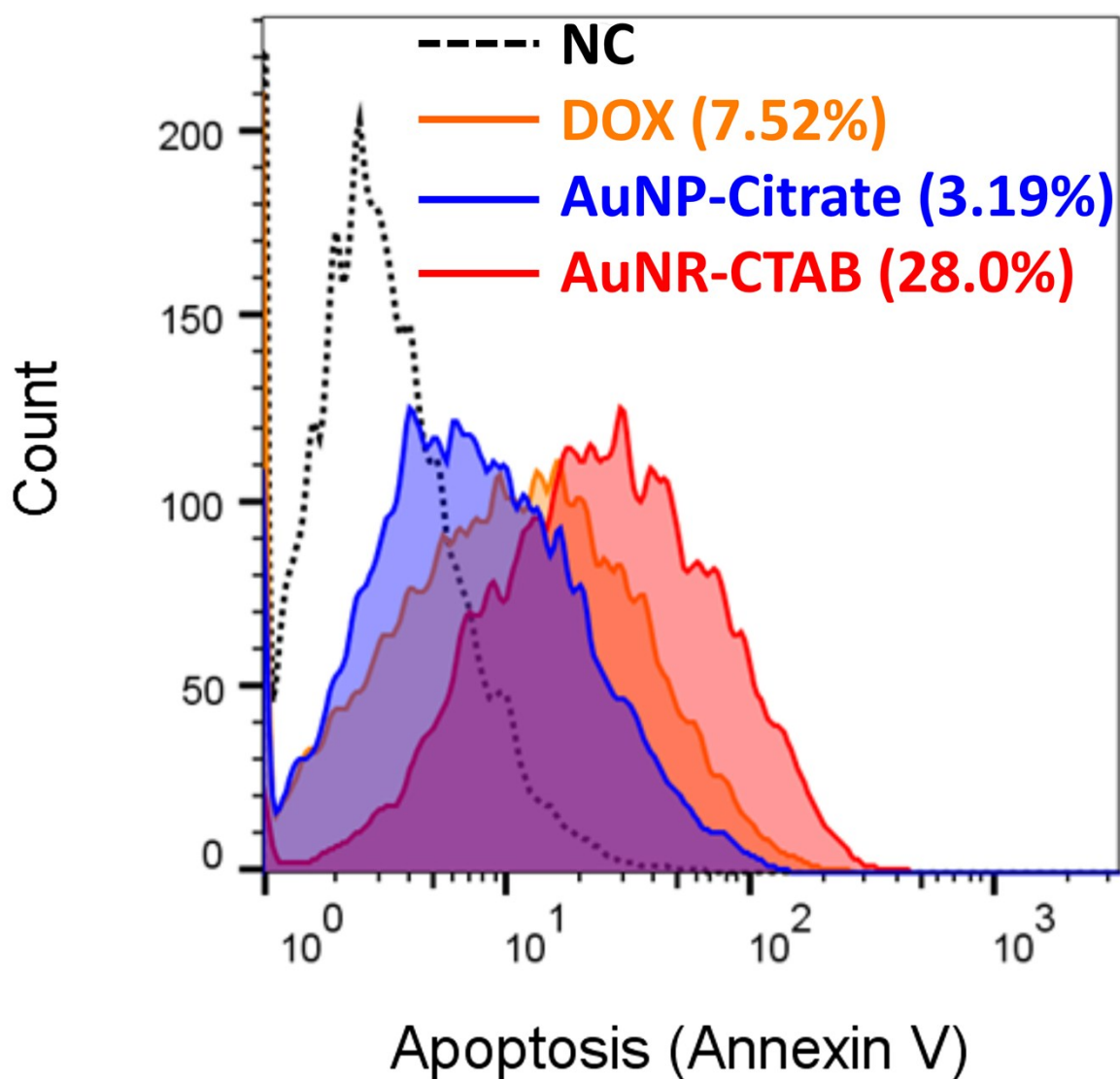


Figure S11. Apoptosis analysis (FACS) following treatment of H1975 cells with anionic AuNP (citrate), cationic AuNR (CTAB), or DOX for 48 hrs.

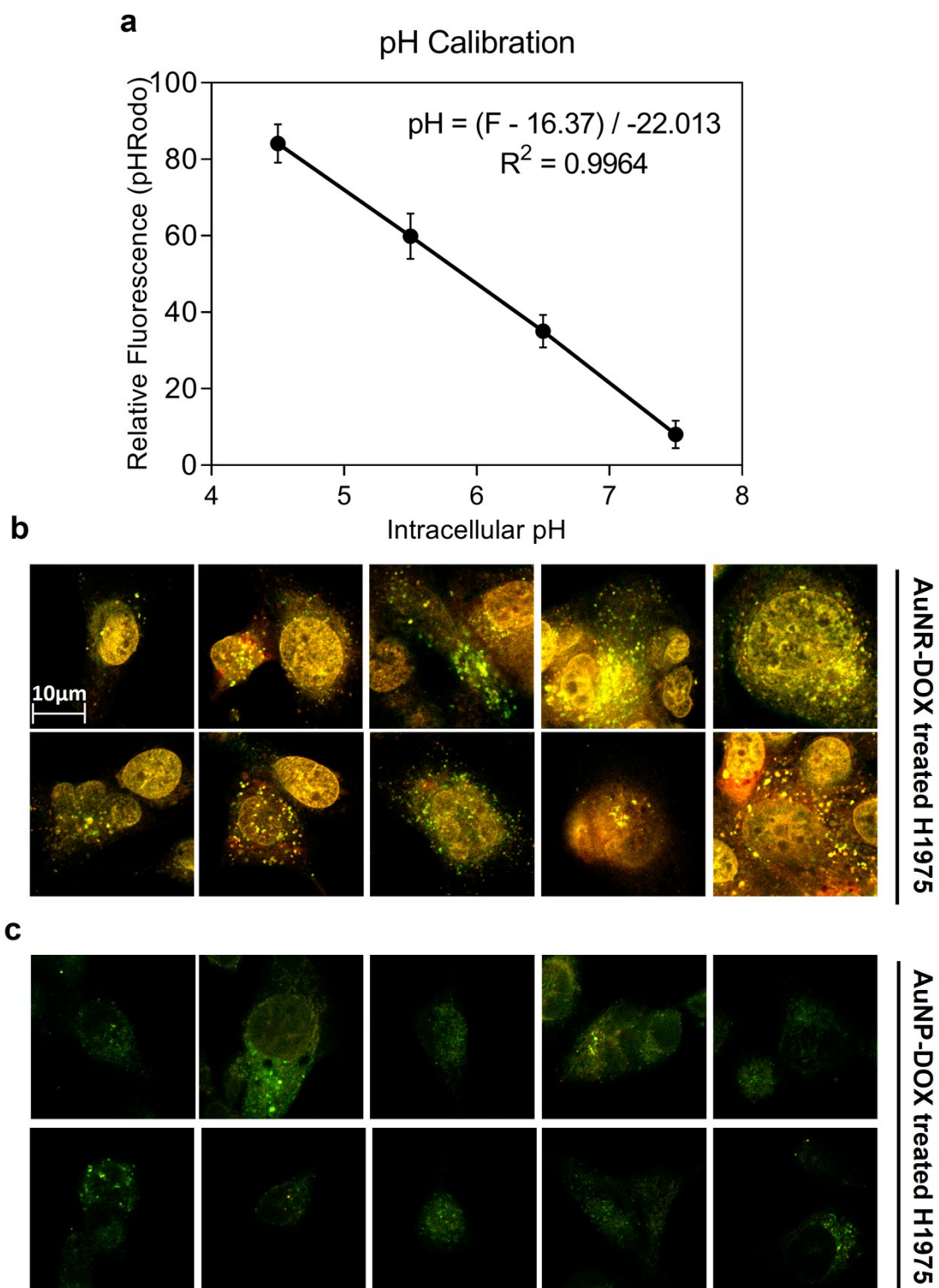
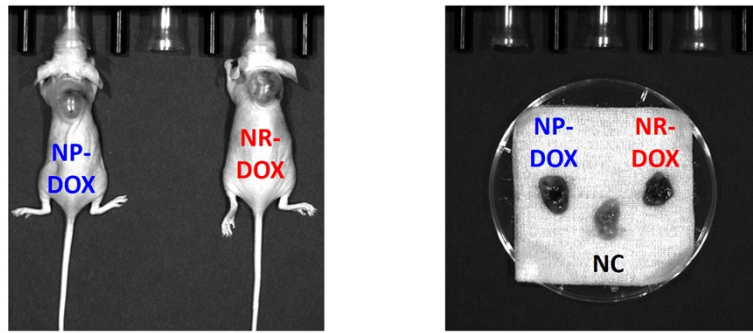


Figure S12. (a) pH calibration curve for intracellular pH of pHRodo stained H1975 cells. (b and c) Additional confocal microscopy images of DOX (red) and pHRodo staining (green) in H1975 cells treated with AuNP-DOX or AuNR-DOX nanoparticles for 24 hrs.



----- NC
—— AuNP-DOX (63.9%)
—— AuNR-DOX (58.3%)

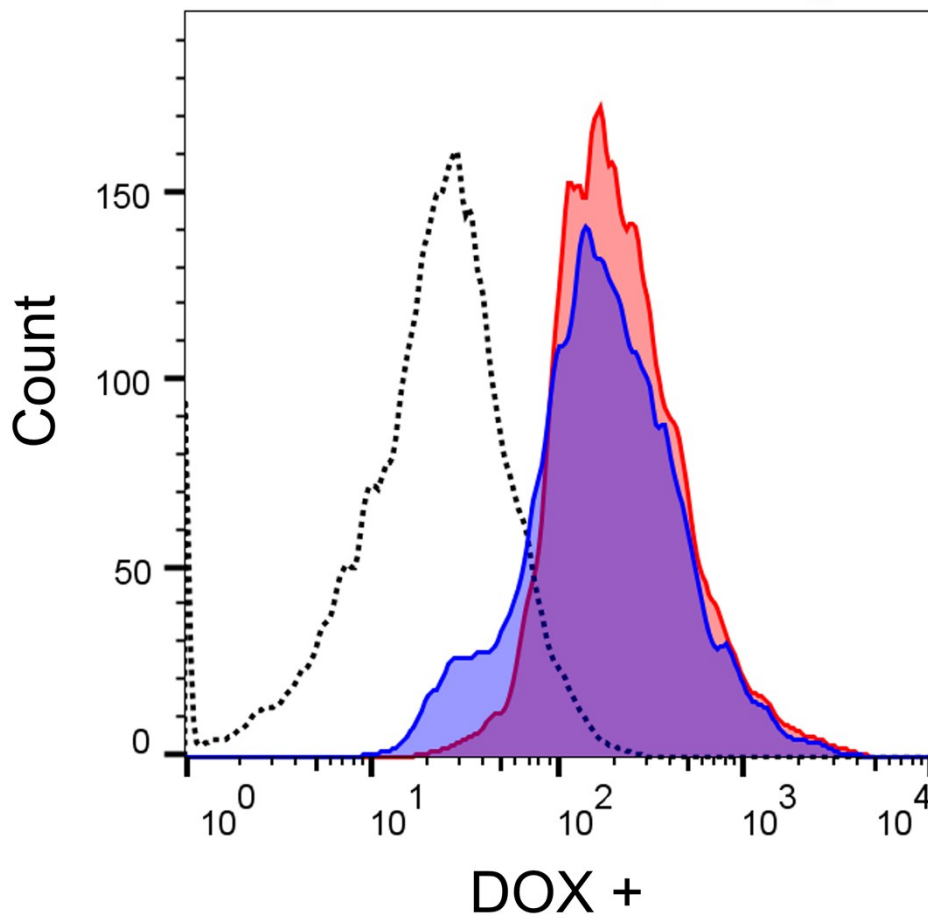


Figure S13. Photograph of H1975 tumor bearing mouse model (left) and *ex-vivo* imaging of tumors (right). DOX uptake analysis (FACS) in H1975 tumor tissues after the direct tumor injection of AuNP-DOX and AuNR-DOX shows identical DOX uptake (after 6 hrs of injection).

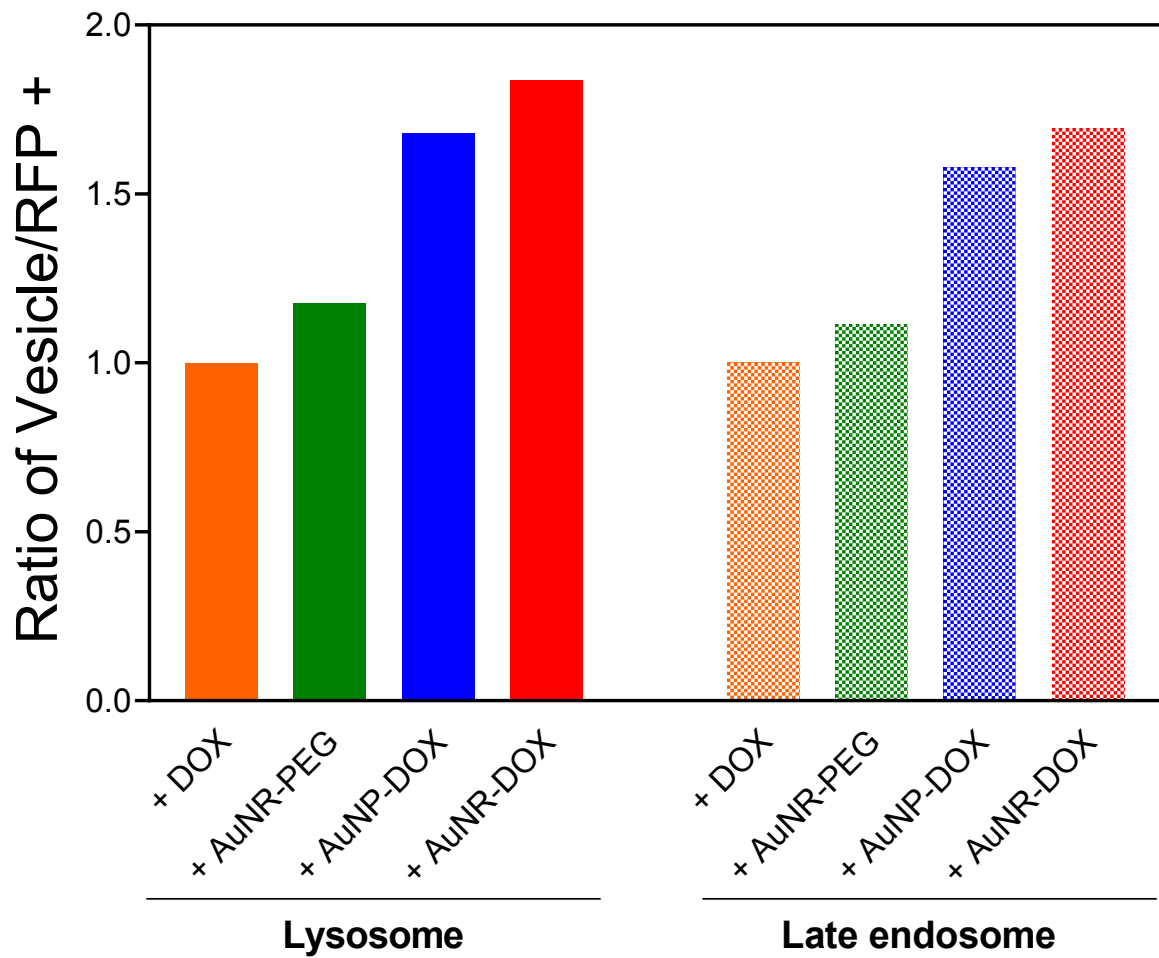


Figure S14. Normalized (to DOX-treated samples) intensity of lysosome (LAMP2) and late endosome (M6PR) vesicles per H1975_{Flu-RFP} cells (FACS analysis) analyzed from xenograft tumor tissues.